ARTICLE IN PRESS

Available online at www.sciencedirect.com

SCIENCE DIRECT®

ELSEVIER

Materials Chemistry and Physics 9712 (2002) 1–7

MATERIALS CHEMISTRY AND PHYSICS

www.elsevier.com/locate/matchemphys

Self-assembled 3D photonic crystals from ZnO colloidal spheres

Eric W. Seelig [a], Alexey Yamilov [b], Hui Cao [b], R.P.H. Chang [a,*]

[a] *Department of Materials Science and Engineering and Materials Research Center, Northwestern University, Evanston, IL 60208, USA*
[b] *Department of Physics and Astronomy and Materials Research Center, Northwestern University, Evanston, IL 60208, USA*

Received 3 June 2002; received in revised form 9 October 2002; accepted 9 October 2002

Abstract

We present a novel method for the controlled synthesis of monodisperse ZnO colloidal spheres. These spheres are self-assembled into fcc periodic arrays. Optical measurements, including reflection-mode optical microscopy and transmission and single-domain reflection spectroscopy, reveal that the periodic arrays exhibit a photonic band gap in the (1 1 1) direction of the fcc lattice, and calculations are presented to estimate the effective value of the refractive index of the colloidal spheres. Finally, photoluminescence (PL) measurements show that the ZnO lasing thresholds are lower in periodic structures than in random arrays of identical spheres.

Keywords: Zinc oxide; Colloidal spheres; Self-assembly; Photonic crystals

1. Introduction

Photonic crystals show a great deal of promise for applications in numerous types of devices in 1, 2, and 3D structures. The simplest devices are 1D structures consisting of alternating layers of high- and low-index materials. By carefully selecting the thickness of the alternating layers and the refractive indices of the materials, the structure can be engineered to reflect a selected range of wavelengths. Structures of this type form the basis for numerous devices including dielectric mirrors and vertical-cavity surface-emitting lasers [1].

2D structures show promise for integration on silicon. One significant problem with the evolution of photonic integrated devices is the ability to produce waveguides that can efficiently move photons across the surface of a chip. Specifically, traditional waveguide designs cannot include sharp bends without significant signal loss. 2D waveguide structures consisting of periodic 2D arrays of columns of a dielectric material have been demonstrated in which light can be efficiently guided around a 90° bend [2]. In addition to passive devices such as waveguides, there is also significant interest in devices formed from 2D periodic structures in optically active materials. Some research has demonstrated that it is possible to form a 2D defect-mode photonic band gap laser in an InGaAs thin film system. A photonic crystal is formed in the active layer by etching a periodic array of holes in the film. A defect is intentionally introduced into the photonic crystal which acts as a laser cavity, and provides the opportunity for coherent feedback [3].

A great deal of work is also underway in the area of 3D photonic crystals. Numerous techniques have been devised in an effort to produce periodic arrays of dielectric materials that can exhibit a photonic stop band. Some synthetic techniques are quite elaborate including complex, multi-layer lithography [4], multi-beam holographic lithography [5], optical interference methods [6], and production of so-called inverted opal structures [7,8]. One of the simplest techniques, however involves colloidal self-assembly [9–11]. Essentially, monodisperse colloidal spheres will spontaneously assemble into periodic arrays under certain circumstances. Self-assembly does have some limitations; for example, colloidal spheres typically arrange into a close-packed FCC array, while it has been calculated that a diamond lattice would be more likely to produce an omnidirectional photonic band gap [12]. Also, thus far, most of the work performed in the area of self-assembled 3D photonic crystals has involved a few materials which are readily available as monodisperse colloidal spheres in sizes appropriate for photonic crystals including SiO_2 and polymers, such as polystyrene and PMMA. While these materials do prove easy to assemble into FCC periodic arrays [11], their refractive indices are relatively low. In addition, while some studies have been performed in which emissive materials are added to the photonic crystal matrix [8,10,13], no work has explored the properties of photonic crystals formed directly from optically active materials.

* Corresponding author. Fax: +1-847-4917820.
E-mail address: r-chang@northwestern.edu (R.P.H. Chang).

0254-0584/02/$ – see front matter © 2002 Published by Elsevier Science B.V.
PII: S0254-0584(02)00492-3

Clearly, there is a great deal of novel work that can be performed in the area of self-assembled 3D photonic crystals simply by choosing different material systems. Van Blaaderen et al. have produced a number of interesting emissive materials as monodisperse colloidal spheres including Er^{3+}-doped SiO_2 [14], dye-doped PMMA [15], and SiO_2/ZnS core/shell structures [16]. ZnO is another promising candidate for optically-active self-assembled photonic crystals because of its interesting optical properties. First, ZnO has a higher refractive index (2.1–2.2 in the visible regime) than other materials (1.4–1.5 for SiO_2 and most polymers). In addition, ZnO has been found to be an efficient emitter, exhibiting lasing behavior in the near UV ($\lambda \sim 385$ nm) [17].

In the current work, we describe 3D photonic crystals formed from ZnO colloidal spheres. We describe the synthetic process used to produce monodisperse ZnO colloidal spheres over a broad range of sizes, and the technique used to produce photonic crystals from these colloids. We also explore the optical properties of our photonic crystals.

2. ZnO colloidal sphere synthesis

The ZnO colloidal spheres used in this work were produced by a reaction similar to that described by Jezequel et al. [18]. ZnO was formed by hydrolysis of zinc acetate dihydrate (ZnAc). In a typical reaction, 0.03 mol ZnAc was added to 300 ml diethylene glycol (DEG). This reaction solution was heated under reflux to 160 °C. Shortly after reaching the working temperature, precipitation of ZnO occurred. Jezequel et al., reported that it was possible to produce monodisperse ZnO powders of various sizes using this method by changing the rate at which the reaction solution was heated. They reported the production of spheres in the narrow size range 0.2–0.35 μm. Powders produced using this technique in our lab, however, were typically widely polydisperse with sizes ranging from ~100 to 1500 nm.

In our experiments monodisperse ZnO colloidal spheres were produced by a two-stage reaction process. A primary reaction was performed as described above, and the product was placed in a centrifuge. The supernatant (DEG, dissolved reaction products, and unreacted ZnAc and water) was decanted off and saved, and the polydisperse powder was discarded. A secondary reaction was then performed to produce the monodisperse ZnO spheres. The secondary reaction began in the same way as a primary reaction: 0.03 mol ZnAc was added to 300 ml DEG and the reaction solution was heated under reflux. Prior to reaching the working temperature, however, typically at 150 °C, some volume of the primary reaction supernatant was added to the solution. Following this addition, there was a temperature drop, and precipitation would typically occur at a lower temperature than without such an addition. After reaching 160 °C, the reaction was stirred for one hour, after which the heat source was removed, and the flask cooled to room temperature.

The scanning electron microscope (SEM) images in Fig. 1 reveal that the ZnO synthesized using this technique consists of monodisperse colloidal spheres, and that the size of the spheres varies inversely and monotonically with the amount

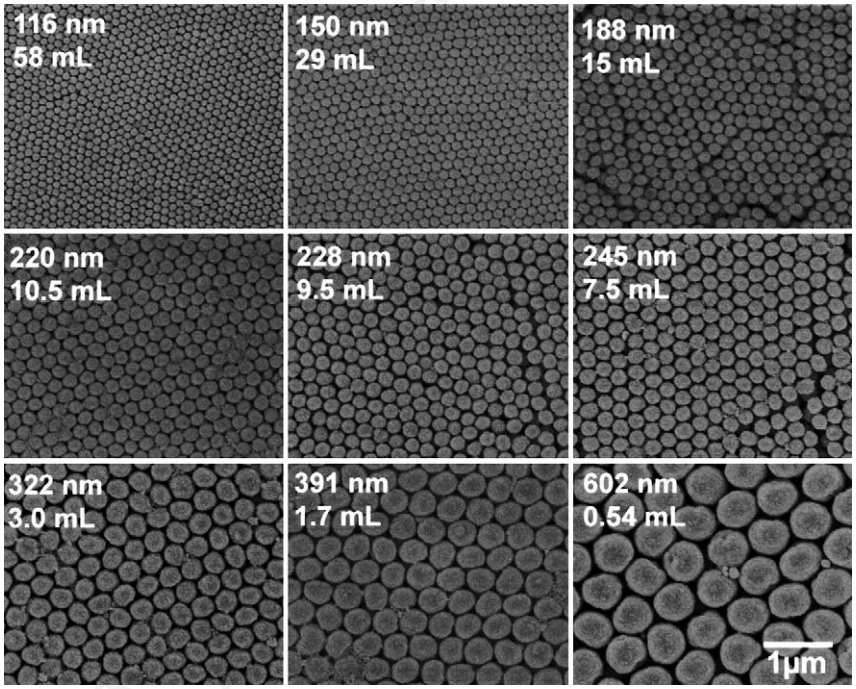

Fig. 1. SEM micrographs of monodisperse ZnO powders of various sizes produced using a two-stage hydrolysis. Numbers in the corners of the images indicate the mean sphere diameter and the amount of primary supernatant added.

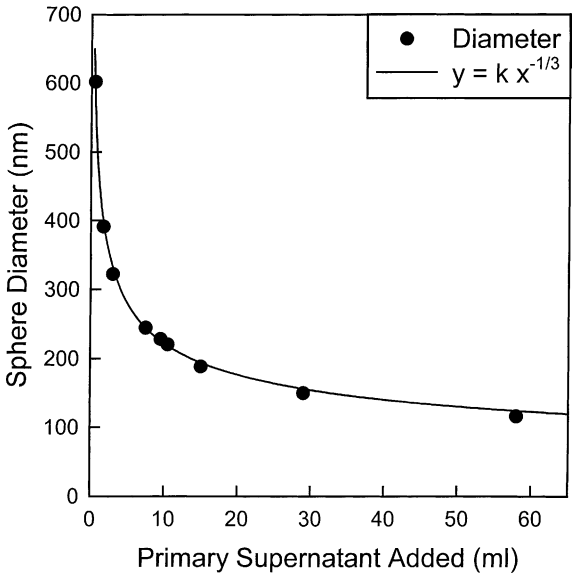

Fig. 2. Plot of the relationship between the amount of primary supernatant added and sphere diameter. Squares indicate real data, and the line is a fit of a function of the form $kx^{-1/3}$.

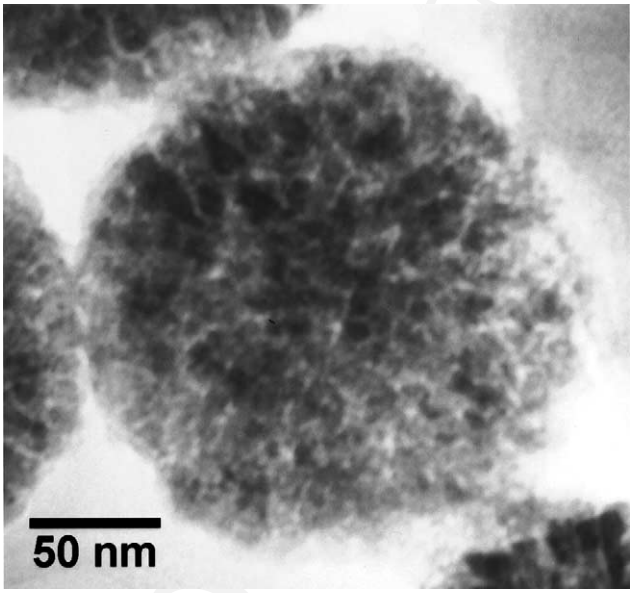

Fig. 3. TEM Micrograph of a single ZnO sphere showing nanocrystalline substructure of the material.

of primary supernatant added. Careful analysis of the micrographs reveals that the spheres formed are monodisperse within 5–8%. Plotting sphere diameter as a function of primary supernatant added reveals that the data fall very close to a $kx^{-1/3}$ dependence, as can be seen from the solid line in Fig. 2. This result provides a method to easily synthesize monodisperse ZnO colloidal spheres over a broad size range (∼100–600 nm), with good control over the diameter. We expect that it should be possible to extend this method to produce particles larger or smaller than those that have been synthesized thus far. As will be seen, however, this range of sizes is adequate to create photonic crystals with band gaps covering the entire visible spectrum and extending well into the UV and IR. In addition to revealing the sphere diameter, SEM also shows that the spheres are made up of numerous nanocrystallites. X-ray diffraction analysis of the colloid reveals that the material is hexagonal ZnO with a crystallite size of 10–20 nm and no preferential growth direction. The transmission electron micrograph in Fig. 3 confirms the polycrystalline nature of the spheres.

It should be noted that it is necessary to use the supernatant from the primary reaction to produce the monodisperse colloidal spheres. If the ZnO is not removed from the reaction solution, the polydisperse spheres from the primary reaction mix with the monodisperse spheres from the secondary reaction, disrupting the self-assembly of the periodic arrays described later. Additionally, if pure DEG is added as the nucleation agent, the product consists of polydisperse ZnO spheres similar to that of the primary reaction. Furthermore, a "synthetic" primary reaction supernatant consisting of amounts of precursor (ZnAc) expected to remain unreacted, and appropriate amounts of soluble reaction by-products (acetic acid) failed to produce monodisperse ZnO spheres.

Photonic crystals were produced from the ZnO colloidal spheres using a sedimentation self-assembly process. The reaction solution was dropped onto a substrate typically at 160 °C, and as the solvent evaporated, the particles spontaneously assembled into periodic structures with domain sizes typically in the range of several microns. Examples of the structures observed can be seen in Fig. 1. Substrates were chosen based upon application. For SEM, Si substrates were used, and for optical measurements, glass substrates were used. From optical microscopy, there is no difference between layers formed on glass and those formed on Si.

Temperature plays an important role in the assembly of periodic structures. A series of several samples of 245 nm ZnO was prepared with sedimentation and drying temperatures ranging from 100 to 300 °C. It was noted that at low temperatures, layers exhibited no periodicity observable in SEM, and at high temperatures, the powder adhered poorly to the substrate. The solvent also appears to play an important role in self-assembly. While layers sedimented from the original reaction solution produce crystalline structures, layers sedimented from other solvents including acetone, water, and several alcohols produced no observable periodic structures. This could be, in part, attributable to the lower boiling points, and consequently lower sedimentation temperatures required, when using solvents other than DEG.

Based on plan-view SEM, it is impossible to determine whether the structure of the photonic crystals is FCC or HCP. In order to determine the structure, cross-sectional SEM samples were prepared, and the edge of the layer was observed. An FCC structure was confirmed by the presence in all samples of (1 0 0) square-lattice planes. In addition, it

was observed that the thickess of the layers, while variable across the surface of the sample, has an average value of approximately 2–3 μm, corresponding well with thicknesses calculated from expected yields. Unfortunately, it proved difficult to observe photonic crystal properties for layers this thin, particularly for films of larger particles that may consist of only 3–4 monolayers. In order to produce thicker layers, the reaction solution was concentrated. The as-synthesized solution was placed in a centrifuge, and the powder was allowed to settle to the bottom. Some fraction (typically 85–90%) of the liquid was then removed, and the powder was redispersed by sonication. A single drop placed on a heated substrate would then result in a much thicker, but still periodic structure.

3. Optical characterization

Several types of measurement were performed in order to characterize the photonic band gap structures in the periodic ZnO arrays. Reflection-mode optical microscopy was used to observe the general color of the reflected light, large area transmission measurements were performed to detect the presence of a photonic stop band, and spatially-resolved reflection spectroscopy was performed to evaluate the quality of individual domains. In addition, we have performed simulations to evaluate the photonic band structure of our crystals.

Using normal-incidence transmission spectroscopy, it was easy to observe band gaps for our periodic structures. The size range of our colloidal spheres resulted in band gaps covering the entire visible part of the spectrum, and are expected to extend from the UV to the IR. Plots of the transmission results and their corresponding particle sizes can be seen in Fig. 4. Table 1 lists the mean sphere diameters,

Table 1
Relationship between ZnO sphere diameter and photonic band gap position

d (nm)	λ (nm)	d/λ
116	257	–
150	333	–
188	433	0.433
220	487	0.452
245	538	0.455
322	700	0.460
391	865	0.452
602	1336	–

the observed wavelength of the corresponding photonic band gap, and the ratio of particle size to wavelength (d/λ). The ratio is constant to within a few percent over all samples. The lighter values in Table 1 correspond to samples whose gap is not observed, but is expected to lie either outside of the range of the spectrometer or beyond the absorption edge of ZnO. It should also be noted that the colors corresponding to the band gaps observed are clearly visible in reflection-mode optical microscopy.

While transmission is an effective technique for detecting the presence and location of a photonic band gap, it is difficult to quantify the width of the gap because it measures a large area of the sample which may include many different periodic photonic domains, as well as areas of disorder and areas where no material is present. In order to better characterize the photonic band gap, spatially-resolved reflection spectroscopy was used [10]. Essentially, a white light source was focused onto the surface of the sample using a microscope objective lens. The image of the sample was then projected on the entrance slit of a spectrometer. Images of the spectrometer CCD were taken, with one dimension corresponding to wavelength and the other corresponding to real space on the surface of the sample. By selecting a few lines

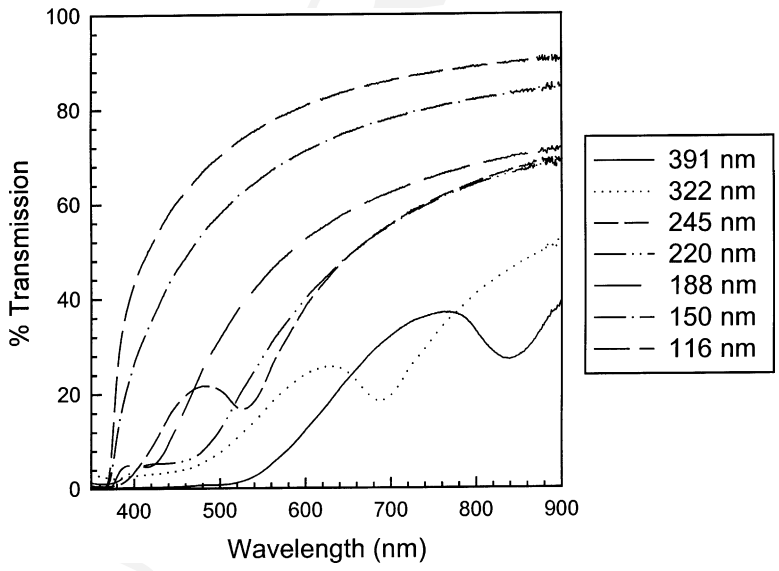

Fig. 4. Transmission spectra for periodic layers of ZnO spheres of various sizes.

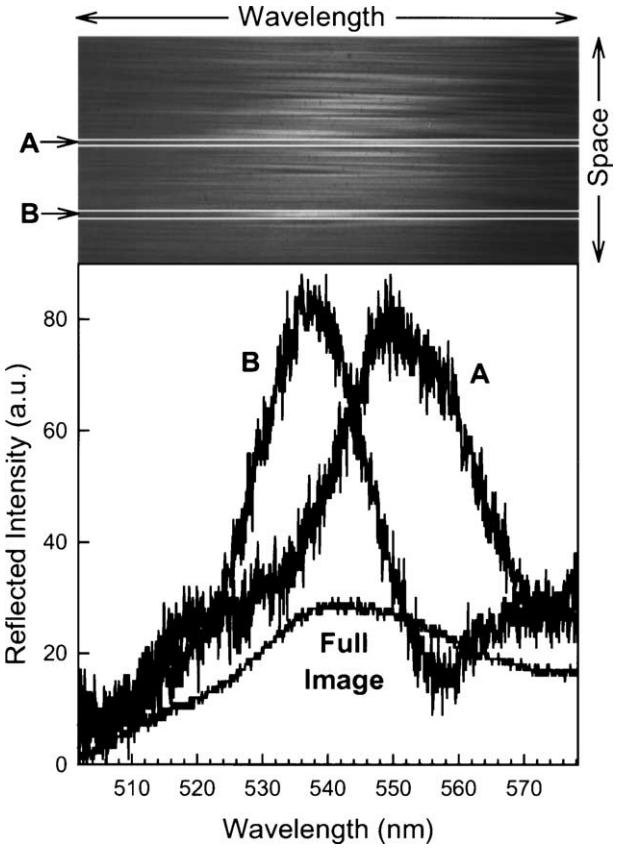

Fig. 5. Spectrometer CCD image and corresponding plots for reflection spectroscopy of a 245 nm ZnO powder structure. Letters beside the image indicate the CCD location from which the corresponding curves in the plot were constructed.

from the spectrometer CCD corresponding to single domains on the surface of the sample, it is possible to get a better measure of both the position and the width of the photonic band gap. Fig. 5 shows a typical spectrometer CCD image for a layer of 245 nm ZnO colloidal spheres and spectra corresponding to both the full image and two single-domain bands. While transmission measurements result in a FWHM of 60–80 nm, and large area reflection measurements show a width of approximately 40 nm, single-domain measurements result in a spectral width of approximately 20 nm or about 4%. It is believed that the broadening of the band gap in large-area cases results from the addition of numerous domains that may have slightly different orientations and therefore slightly different reflection maxima. This is clear from the different positions of the two single-domain plots show in Fig. 5.

To support our optical measurements we have also performed band structure calculations. Using a block-iterative, frequency-domain method [19] for Maxwell's equations (in a plane-wave basis) we calculated the band structure for 3D FCC lattices of dielectric spheres with indexes of refraction varying between 1.2 and 3.0, and radius to interparticle distance ratios (r/d, a measure of the packing density of the spheres) from 0.2 to 0.6. To describe normal-incidence optical experiments, we restricted ourselves to the (1 1 1) direction of the FCC lattice. The results of these calculations can be found in Fig. 6. Fig. 6a shows a plot of gap position (d/λ) in the (1 1 1) direction and 6(b) a plot of the gap width (%) normalized by the center frequency, each as a function of refractive index and r/d. For a refractive index of 2.1 (approximate bulk value for ZnO) the results indicate that d/λ can be approximated as 0.35, while in our case the ratio was close to 0.45. This discrepancy implies that the effective refractive index of the photonic crystal structure differs significantly from the bulk value. Packing density was estimated from SEM images to yield r/d in the 0.45–0.50 range. Restricting the packing parameter to this interval, and keeping $d/\lambda = 0.45$ (bold segment on Figs. 6a,b), gives us an effective index in the 1.5–1.7 range. This value is further supported by the calculations of relative gap width. As can be found in Fig. 6b, the width is predicted to lie between 5.5 and 7.8%. The value observed in our single-domain reflection measurements, approximately 4%, is smaller than the above prediction. This reflects the presence of the residual disorder, inevitable in the experimental photonic crystal structures studied here.

The fact that the refractive index is lower than the bulk value is most likely the result of low density in the powders. Jezequel et al., found that ZnO spheres produced by the hydrolysis of ZnAc are highly porous [18]. It may be possible to increase the refractive index by annealing the powders to increase their density, or by filling in the pores with SiO_2 in a technique similar to that described by Velikov and van Blaaderen [16].

In addition to the optical measurements used to characterize the photonic band gap, photoluminescence (PL) measurements were also performed to observe the emissive properties of the colloidal spheres. In these measurements, a pulsed, frequency-tripled, Nd:YAG laser emitting at 355 nm at 10 Hz with a pulse length of approximately 20 ps was used as the pump source. The beam was focused to a spot approximately 25 μm in diameter on the surface of the sample. The PL system was set up with a white light source and a CCD camera to observe the samples and select a clean area on the surface for measurement. In addition, the sample could be viewed after the PL experiments were complete to see if any damage had been caused by the pump source.

For the lasing measurements, 16 samples were prepared comprising periodic and random structures in each of eight different colloidal sphere sizes. All samples exhibited lasing type behavior, detectable by the evolution of narrow peaks in the emission spectrum. For each sample, several locations were measured, and the value of the lasing threshold was recorded. In all cases, periodic structures showed a lower lasing threshold by a factor ranging from ∼1.5 to 4.0 with an average value of approximately 2.5. This behavior is likely due, at least in part, to a higher sphere packing density in the periodic structures. In future work, we plan to produce a photonic crystal in which the position of the pho-

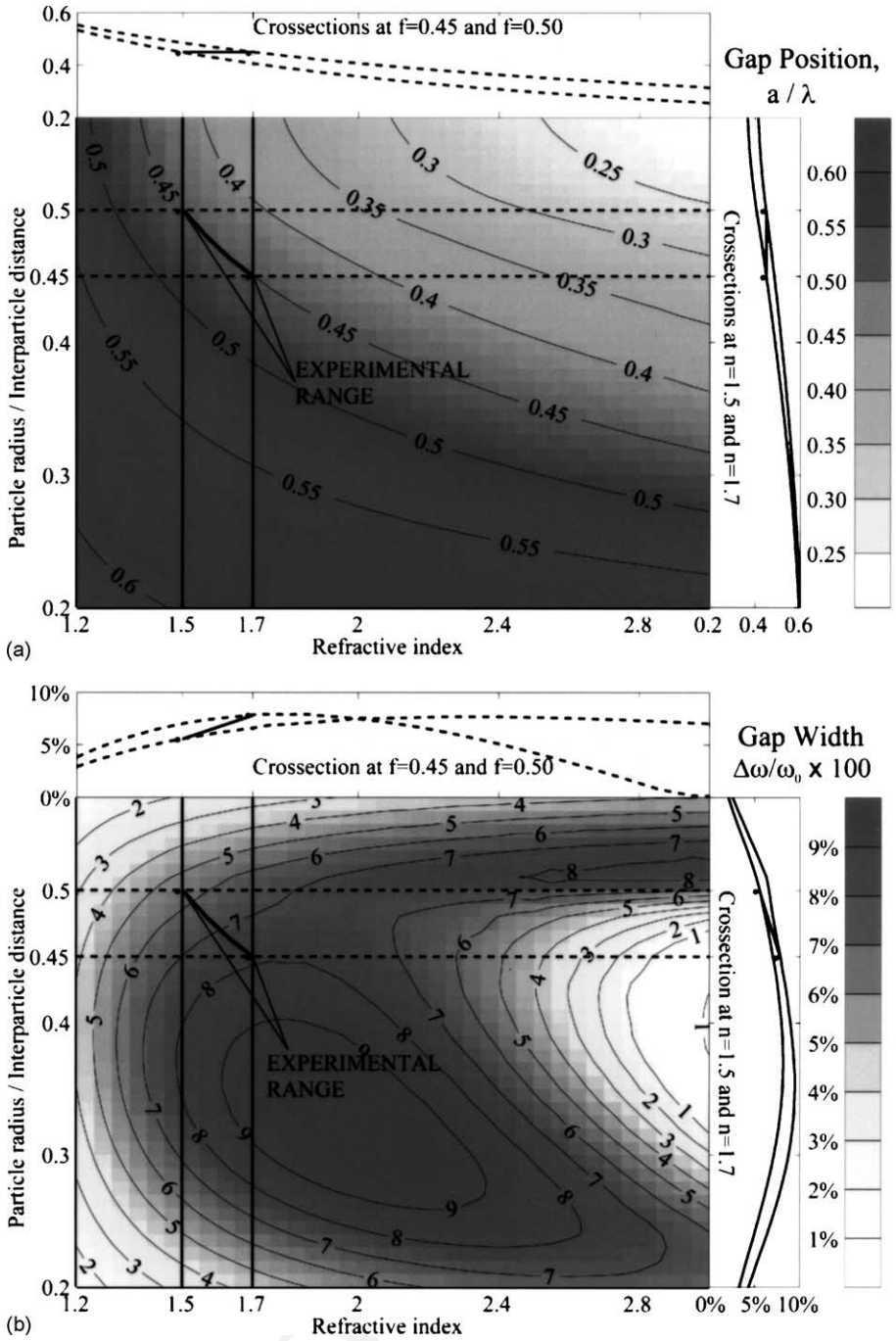

Fig. 6. Results of photonic band calculations. (a) Gap position (d/λ) and (b) gap width (%) as a function of refractive index and packing density.

tonic band gap overlaps the ZnO emission spectrum which we expect will demonstrate a significantly higher lasing efficiency.

4. Conclusions

In summary, we have developed a technique to produce monodisperse ZnO colloidal spheres. Our technique employs a two-step reaction, and allows close and predictable control of the size of the spheres during the secondary reaction by varying the amount of primary reaction supernatant added. We have demonstrated the production of particles ranging in size from ~100 to 600 nm, and believe that it should be possible to go beyond this range.

We have self-assembled periodic arrays of these colloidal spheres by dropping the reaction solution onto substrates and evaporating the solvent. We have found that ordering only occurred at relatively high substrate temperatures, and no ordering could be observed when the reaction solvent

was exchanged for other solvents such as water, acetone, or alcohols.

It has been found that the periodic arrays of the powder exhibit a photonic band gap in the fcc (1 1 1) direction at approximately 2.2d where d is the mean particle diameter. To our knowledge, this is the first demonstration of 3D photonic crystals in ZnO.

Finally, we have performed photoluminescence measurements on random and periodic arrays of layers of our monodisperse colloidal spheres. We have found that the ZnO colloidal spheres are optically active, and capable of exhibiting laser-like behavior. It is found that the lasing threshold in periodic structures is lower than that in random structures by a factor of approximately 2.5.

Because of ZnOs unique optical and lasing properties, this work opens up many unique and exciting research opportunities previously unavailable in the area of self-assembled 3D photonic crystals.

Acknowledgements

This work is supported by the National Science Foundation under grant number ECS-9877113 and by the Northwestern University Materials Research Science and Engineering Center.

References

[1] A. Polman, P. Wiltzius, MRS Bull. 26 (2001) 608.
[2] T. Zijlstra, E. van der Drift, M.J.A. de Dood, E. Snoeks, A. Polman, J. Vac. Sci. Technol. B 17 (1999) 2734.
[3] O. Painter, R.K. Lee, A. Scherer, A. Yariv, J.D. O'Brien, P.D. Dapkus, I. Kim, Science 284 (1999) 1819.
[4] S. Noda, MRS Bull. 26 (2001) 618;
S.Y. Lin, J.G. Fleming, E. Chow, MRS Bull. 26 (2001) 627.
[5] A.J. Turberfield, MRS Bull. 26 (2001) 632.
[6] T. Kondo, S. Matsuo, S. Juodkazis, H. Misawa, Appl. Phys. Lett. 79 (2001) 725.
[7] J. Wijnhoven, W.L. Vos, Science 281 (1998) 802;
A. Blanco, E. Chomski, S. Grabtchak, M. Ibisate, S. John, S.W. Leonard, C. Lopez, F. Meseguer, H. Miguez, J.P. Mondia, G.A. Ozin, O. Toader, H.M. van Driel, Nature 405 (2000) 437;
V. Yannopapas, N. Stefanou, A. Modinos, Phys. Rev. Lett. 86 (2001) 4811.
[8] S.G. Romanov, T. Maka, C.M.S. Torres, M. Muller, R. Zentel, Appl. Phys. Lett. 79 (2001) 731.
[9] G. Subramania, R. Biswas, K. Constant, M.M. Sigalas, K.M. Ho, Phys. Rev. B 6323 (2001) 5111;
H. Miguez, F. Meseguer, C. Lopez, A. Blanco, J.S. Moya, J. Requena, A. Mifsud, V. Fornes, Adv. Mater. 10 (1998) 480;
B. Gates, Y. Xia, Appl. Phys. Lett. 78 (2001) 3178;
G. Subramanian, V.N. Manoharan, J.D. Thorne, D.J. Pine, Adv. Mater. 11 (1999) 1261.
[10] Y.A. Vlasov, M. Deutsch, D.J. Norris, Appl. Phys. Lett. 76 (2000) 1627.
[11] S.H. Park, Y.N. Xia, Langmuir 15 (1999) 266.
[12] J.D. Joannopoulos, R.D. Meade, J.N. Winn, Photonic crystals: molding the flow of light, Princeton University Press, Princeton, NJ, 1995.
[13] Y.A. Vlasov, N. Yao, D.J. Norris, Adv. Mater. 11 (1999) 165;
E.P. Petrov, V.N. Bogomolov Kalosha Jr., S.V. Gaponenko, Phys. Rev. Lett. 81 (1998) 77.
[14] M.J.A. de Dood, B. Berkhout, C.M. van Kats, A. Polman, A. van Blaaderen, Chem. Mater. 14 (2002) 2849.
[15] G. Bosma, C. Pathmamanoharan, E.H.A. de Hoog, W.K. Kegel, A. van Blaaderen, H.N.W. Lekkerkerker, J. Colloid Interface Sci. 245 (2002) 292.
[16] K.P. Velikov, A. van Blaaderen, Langmuir 17 (2001) 4779.
[17] H. Cao, Y.G. Zhao, X. Liu, E.W. Seelig, R.P.H. Chang, Appl. Phys. Lett. 75 (1999) 1213;
H. Cao, J.Y. Xu, E.W. Seelig, R.P.H. Chang, Appl. Phys. Lett. 76 (2000) 2997;
H. Cao, J.Y. Xu, D.Z. Zhang, S.H. Chang, S.T. Ho, E.W. Seelig, X. Liu, R.P.H. Chang, Phys. Rev. Lett. 84 (2000) 5584;
H. Cao, Y.G. Zhao, S.T. Ho, E.W. Seelig, Q.H. Wang, R.P.H. Chang, Phys. Rev. Lett. 82 (1999) 2278.
[18] D. Jezequel, J. Guenot, N. Jouini, F. Fievet, Mater. Sci. Forum 1994 (1994) 339.
[19] S.G. Johnson, J.D. Joannopoulos, Opt. Express 8 (2001) 173;
K. Busch, S. John, Phys. Rev. E 58 (1998) 3896.